SEMARAK ILMU PUBLISHING

Journal of Advanced Research in Applied Sciences and Engineering Technology

Journal homepage:
https://semarakilmu.com.my/journals/index.php/applied_sciences_eng_tech/index
ISSN: 2462-1943


# Q-Switched Erbium-Doped Fiber Laser Generation using Titanium Aluminum Carbonitride Ti3Al(C0.5N0.5)2 Saturable Absorber

Shairazi Akmal Anuar[1,2], Mohd Fauzi Ab Rahman[2,*], Amal Muaz Nasir[1,2], Anas Abdul Latiff [1], Afiq Arif Aminuddin Jafry[3]

[1] Faculty of Electronic and Computer Engineering, Universiti Teknikal Malaysia Melaka, 76100 Hang Tuah Jaya, Melaka, Malaysia
[2] Fakulti Teknologi Kejuruteraan Elektrik dan Elektronik, Universiti Teknikal Malaysia Melaka, 76100 Melaka, Malaysia
[3] School of Pre-University Studies, Taylor's College, Lakeside Campus, No. 1, Jalan Taylor's, 47500 Subang Jaya, Selangor, Malaysia

**ARTICLE INFO**

***Article history:***
Received 30 January 2023
Received in revised form 17 May 2023
Accepted 25 May 2023
Available online 14 June 2023

***Keywords:***
Fiber laser; Q-Switching; passive technique; pulsed laser

**ABSTRACT**

A new MAX-phase-based saturable absorber (SA) known as Titanium Aluminium Carbonitride, $Ti_3Al(C_{0.5}N_{0.5})_2$ PVA composite film is successfully developed to demonstrate a reliable Q-switched laser in the 1.55-micron region. The $Ti_3Al(C_{0.5}N_{0.5})_2$ composite film with a size of about 1 $mm^2$ is sandwiched between two fibre ferules and integrated into an erbium-doped fibre laser (EDFL) ring cavity. The film SA has a linear absorption of about 5.7 dB at the pulsing region, and a modulation depth of 21%. The Q-switched laser, which is centred at 1561 nm, stably appears at a pump power range of 25 mW-55 mW. The Q-switched laser has the highest repetition rate of 46.3 kHz and the narrowest pulse width of 6.6 µs. The maximum calculated peak power is 1.6 mW, while the highest pulse energy is 10.54 nJ. This demonstration suggests that the $Ti_3Al(C_{0.5}N_{0.5})_2$ can be an alternative SA that may have a good prospect in optical-related applications.

## 1. Introduction

Pulsed fiber lasers have unique properties such as the ability to resist disturbance, highly narrow and adjustable beam quality, great stability, excellent flexibility, and considerably high energy conversion efficiency [1]. Due to these reasons, pulsed lasers have been employed in various applications including optical communications, spectroscopy, surgery, remote sensing, and material processing [2]. The pulsed laser can be generated through two primary methods: Q-switching and mode-locking [3]. These methods can be further divided into two categories: active modulation, which involves the employment of an electrically powered modulator to periodically switch loss in the cavity. The other one is passive modulation, which integrates a saturable absorber (SA) within the cavity for modulating loss and energy in the cavity. Additionally, there are two kinds of SAs for the passive creation of pulsed lasers: SA that uses nonlinear or birefringent effect, such as the Kerr lens, nonlinear polarization rotation (NPR) scheme, and nonlinear optical mirror (NOLM); while the

* *Corresponding author.*
*E-mail address: mfauziar@utem.edu.my*

https://doi.org/10.37934/araset.31.1.144155

other type of SA includes semiconductor saturable absorber mirror (SESAM), a short length of doped fibers [4] and two-dimensional (2D) materials. The NPR, NOLM, and SESAM have some limitations associated with narrowly operated bandwidth, intricate construction, susceptibility to ecological variation, and packaging problem. Additionally, the use of the short fiber as SA has issues related to relatively expensive costs and requires unique fabrication facilities.

Nanomaterials have numerous advantages over traditional materials due to their unique properties at the nanoscale which include enhanced properties, improved performance, increased efficiency, better durability, and reduced waste. Overall, nanomaterials have a wide range of applications and are being increasingly used in many areas of science and technology [5–7]. From the perspective of photonics, the 2D nanomaterial based SAs have aroused great interest recently due to their exceptional optoelectronic properties and strong quantum confinement. These include the demonstration of graphene [8], topological insulators (TIs) [9], transition metal dichalcogenides (TMDCs) [10], black phosphorus (BP) [11], and transition metal oxides (TMO) [12,13] for pulsed laser generation. Recently, the research in MXene-based SAs has gained extensive attention due to their excellent nonlinear optical properties [1,14–16]. The general formula for the MXene is $M_{n+1}X_nT_x$, where M represents the 2D transition metal, X represents carbon or nitrogen, and T belongs to the face termination element, including hydroxyl, oxygen, or fluorine, with x denotes the number of terminal groups. However, the study of their predecessor, MAX-phase-based SA, typically for the generation of pulsed fiber laser has not been fully explored. To be more specific, the MAX phase is an early form of MXene, before the removal of the termination group, such as Aluminum. The MAX phase has an outstanding melting temperature, excellent corrosion resistance, high elastic modulus at room temperature, low density, excellent oxidation resistance as well as good thermal and electrical conductivity [15,17]. Due to the aforementioned reasons, certain MAX phase-based SAs [15,17,18] have been demonstrated for the generation of reliable pulsed lasers.

In this work, we demonstrate Q-switched pulse generation using a MAX phase, Titanium Aluminum Carbonitride $Ti_3Al(C_{0.5}N_{0.5})_2$ SA. It is obtained by combining the compound with PVA to form a composite film SA using a solution drop casting approach. The approach is easy and requires less cost and simple lab equipment. The $Ti_3Al(C_{0.5}N_{0.5})_2$ – PVA composite film SA is incorporated into an erbium-doped fiber laser (EDFL) ring cavity to function as a Q-switcher. The SA device forms a stable single wavelength Q-switched laser that peaks at 1561 nm, with the highest achievable pulse frequency of 46.3 kHz and pulse width of 6.6 µs. The fabricated $Ti_3Al(C_{0.5}N_{0.5})_2$ SA inherits metal and ceramic properties that are excellent in the aspects of strength, machinability, stiffness, oxidation resistance, high-temperature handling, as well as thermal and electric conductivity. Furthermore, the presence of a considerably good modulation depth of 21% shows the potential of the SA to facilitate pulsed laser. To our knowledge, this is the first time, the $Ti_3Al(C_{0.5}N_{0.5})_2$ material is used to induce the Q-switching operation particularly at the 1.5-micron regime.

## 2. SA Fabrication and Characterization

The synthesis of the $Ti_3Al(C_{0.5}N_{0.5})_2$ -PVA film as shown in Figure 1, involves the solution drop-casting technique, where the mix-solution is poured into a clean petri dish. Then the solution is left to evaporate for two days, to form a composite film SA. The mentioned techniques are relatively simple, practical, and cheap, as they do not require precise control and highly modern fabrication tools. First, 0.5 g of $Ti_3Al(C_{0.5}N_{0.5})_2$ compound powder with a phase purity of about 98% (from Laizhou Kai Kai Ceramic Materials), was weighed and put into a beaker. Then, 0.5 g of polyvinyl alcohol (PVA) powder was mixed with 60 ml of deionized water in another beaker and stirred at 90 °C for three hours until it was harmoniously dissolved. The advantages of using the PVA as a host film include

nontoxic, cheap, good film formation, superior mechanical, and good thermal properties, as well as improved interfacial adhesion with reinforcing materials like fibers. Additionally, embedding the $Ti_3Al(C_{0.5}N_{0.5})_2$ into the PVA host would secure the material components from perturbation that could degrade the SA performance. Next, the $Ti_3Al(C_{0.5}N_{0.5})_2$ -PVA composite precursor solution was synthesized by mixing the polymer solution with the $Ti_3Al(C_{0.5}N_{0.5})_2$ powder. The powder was entirely dissolved after being agitated using a magnetic stirrer for 24 hours at room temperature. The solvent was then put into an ultra-sonification bath for 100 minutes. Later, the precursor solution was stirred again for 24 hours. Finally, the $Ti_3Al(C_{0.5}N_{0.5})_2$ -PVA film was obtained by pouring the precursor solution into a petri dish and allowing it to dry for 48 hours in an air purifier.

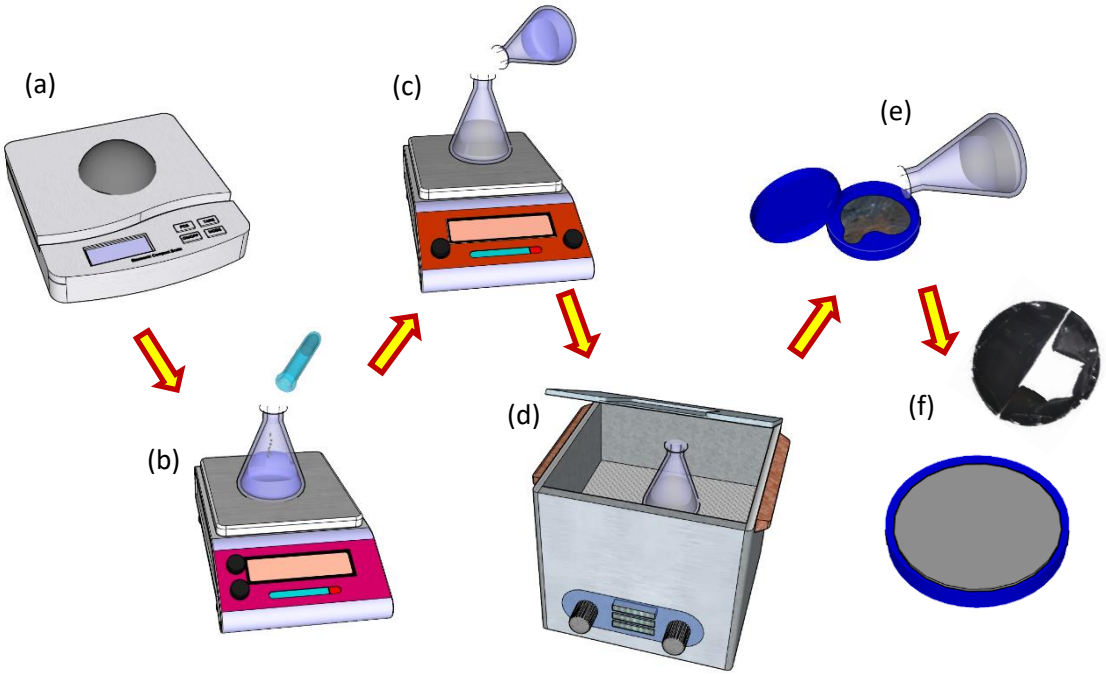


**Fig. 1.** The fabrication process of $Ti_3Al(C_{0.5}N_{0.5})_2$ film SA (a) weighing $Ti_3Al(C_{0.5}N_{0.5})_2$ fine powder (b) production process of PVA solution (c) Mix $Ti_3Al(C_{0.5}N_{0.5})_2$ powder with the PVA solution and then followed with the stirring process (d) ultrasonication process (e) drop the precursor solution on petri dish (f) drying phase to produce $Ti_3Al(C_{0.5}N_{0.5})_2$ - PVA thin film

Figure 2 shows the energy dispersive spectroscopy (EDS) spectrum of the fabricated film consisting of $Ti_3Al(C_{0.5}N_{0.5})_2$ and PVA film SA. As shown in the inset of Figure 2, the film SA has a composition of Carbon, C (46.89%), accompanied by Nitrogen (1.51%), Oxygen, O (36.68%), Titanium, Ti (11.50%), and Aluminum, Al (3.42%). A considerably high margin of C and O recorded in the EDS profile is due to the presence of these elements in the composite-based $Ti_3Al(C_{0.5}N_{0.5})_2$ -PVA.

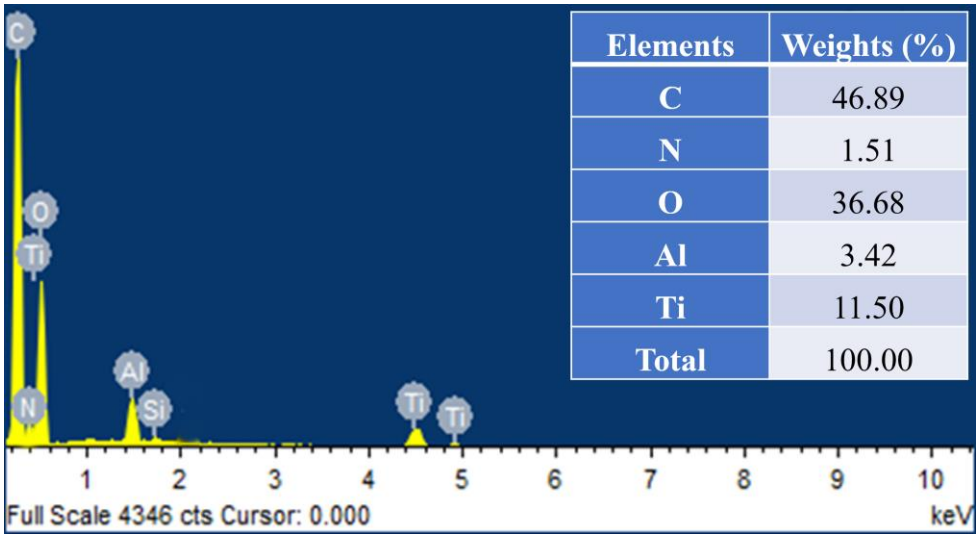


| Elements | Weights (%) |
|---|---|
| C | 46.89 |
| N | 1.51 |
| O | 36.68 |
| Al | 3.42 |
| Ti | 11.50 |
| Total | 100.00 |

**Fig. 2.** EDS spectrum of the $Ti_3Al(C_{0.5}N_{0.5})_2$ – PVA film SA

Figure 3 shows the morphological image of the film surface at a ten µm scale. The SA material is found to be irregular in shape and scattered over the entire film. Figure 4 shows the fabricated SA film (cut in half), with a semi-transparent grey color.

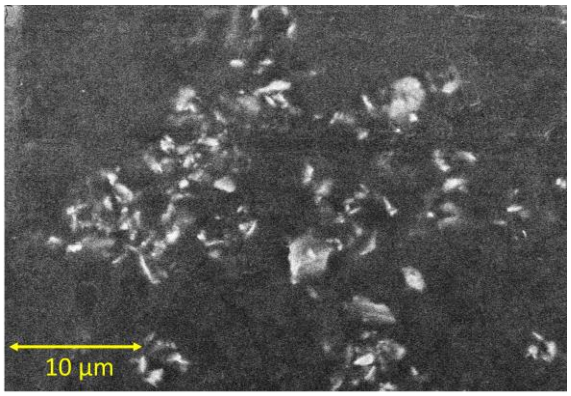


**Fig. 3.** FESEM image of the $Ti_3Al(C_{0.5}N_{0.5})_2$ – PVA film at ten µm scale

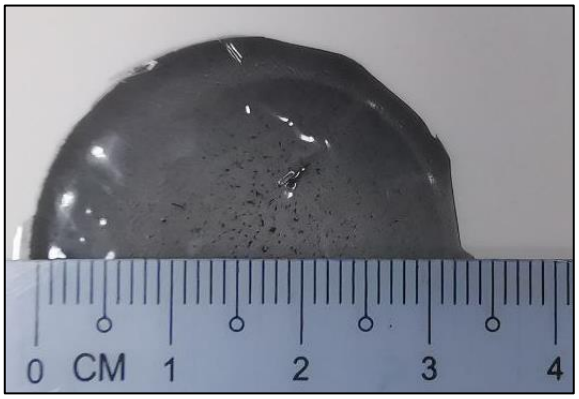


**Fig. 4.** Half-cut semi-transparent image of the $Ti_3Al(C_{0.5}N_{0.5})_2$ – PVA film SA

The $Ti_3Al(C_{0.5}N_{0.5})_2$ SA's linear absorption profile (LAP), taken within a range of 1500 -1600 nm, is shown in Figure 5. As can be seen, about 5.7 dB is absorbed by the film SA at the operating Q-switched laser (1561 nm). The white light source (WLS) emits low-intensity light, which then travels into the film SA; where 5.7 dB is absorbed, while the rest is analyzed by an optical spectrum analyzer (OSA).

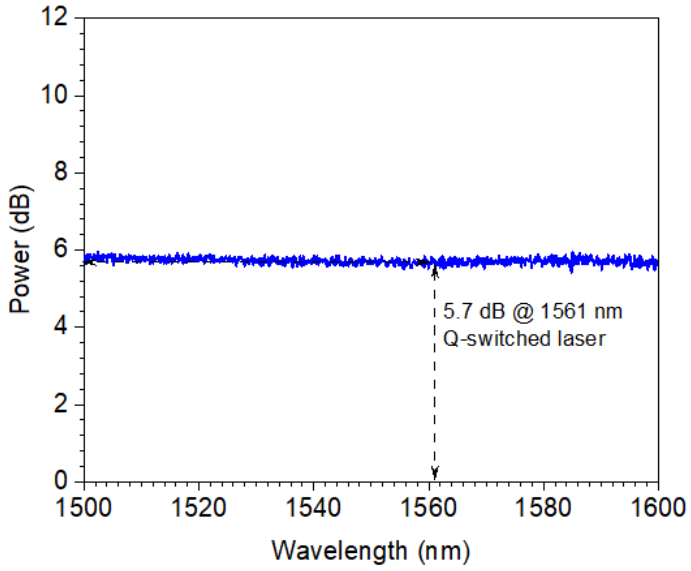


**Fig. 5.** $Ti_3Al(C_{0.5}N_{0.5})_2$ SA linear absorption profile

As shown in Figure 6, the SA has a considerably good modulation depth (transmittance, $\Delta T$) of 21% and a quite low saturation intensity, $I_{sat}$ of 2.1 MW/cm$^2$, while the non-saturable loss, $\alpha_{ns}$ is about 61%. The $\alpha_{ns}$ is high due to high scattering loss, which is caused by the surface roughness, a scattered composite, and uneven film thickness. The plotted nonlinear optical profile is attained by fitting the measured transmission data against the intensity-dependent absorption equation as provided in the inset of Figure 6. In comparison, our fabricated SA has a relatively higher modulation depth than certain SAs [19–21] with considerably low saturation intensity.

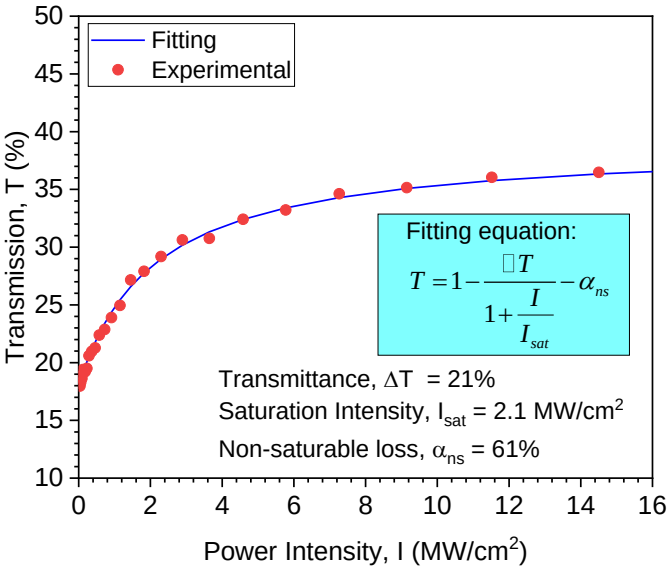


**Fig. 6.** $Ti_3Al(C_{0.5}N_{0.5})_2$ SA nonlinear optical characteristic

## 3. Fiber Laser Cavity Configuration

The configuration of the laser cavity with the in-placed $Ti_3Al(C_{0.5}N_{0.5})_2$ SA is shown in Figure 7. The $Ti_3Al(C_{0.5}N_{0.5})_2$ SA is integrated by sandwiching a tiny piece of $Ti_3Al(C_{0.5}N_{0.5})_2$ SA (~1 mm x 1 mm in size) between two ferrules of patch cords. Before placing the SA film, a small amount of index-

matching gel is applied on the ferrule surface, to reduce optical scattering. The gain medium consisting of 2.4 m long erbium-doped fiber (EDF) is optically pumped by a 980 nm laser diode through a 980/1550 nm wavelength division multiplexer (WDM). The EDF has a core diameter size of 4 µm, a numerical aperture of 0.24, and a core absorption of 24 dB/m at 1550 nm. The optical isolator permits light to be transmitted in uni-direction. The 90/10 coupler diverts 10% of the output for various optical measurements while ensuring 90% of the output is circulated back into the ring cavity. The measurement of the pulse train and RF spectrum is recorded by a digital oscilloscope with an RF spectrum analyzer built-in function (GWINSTEK, MDO-2302AG), while the laser spectrum is observed via an optical spectrum analyzer (Anritsu, MS9740A). These measurements are supported by a high-gain and low-noise photodetector (PD, InGaAs) that converts the optical signal into the corresponding electrical signal. The pulsed laser output power is monitored by a power meter (ILX Lightwave OMM-6810B).

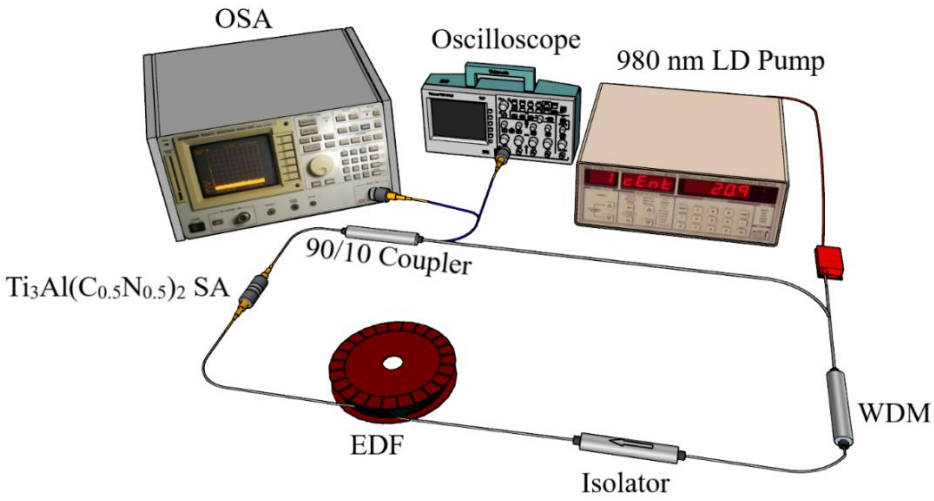


**Fig. 7.** The schematic arrangement of the Q-switched EDFL

## 4. Q-switched Laser Performance

We investigated the Q-switched laser as the $Ti_3Al(C_{0.5}N_{0.5})_2$ SA device inserted into the ring cavity. The Q-switched laser started at an initial repetition rate of 25.6 kHz when the pump power raised to the threshold pump power of 25 mW. The Q-switched laser stably remained as the pump power further increased up to 55 mW. As depicted in Figure 8, the repetition rate increases almost linearly from 25.6 kHz to 46.3 kHz at the ascending pump power (25 mW to 55 mW). On the other hand, the pulse width narrows from 17.8 µs to 6.6 µs, due to a gain compression that occurs in the laser cavity as the pump power is enhanced. Moreover, higher pump power contributes to a faster SA saturation, because of the population inversion which repeats in a faster manner.

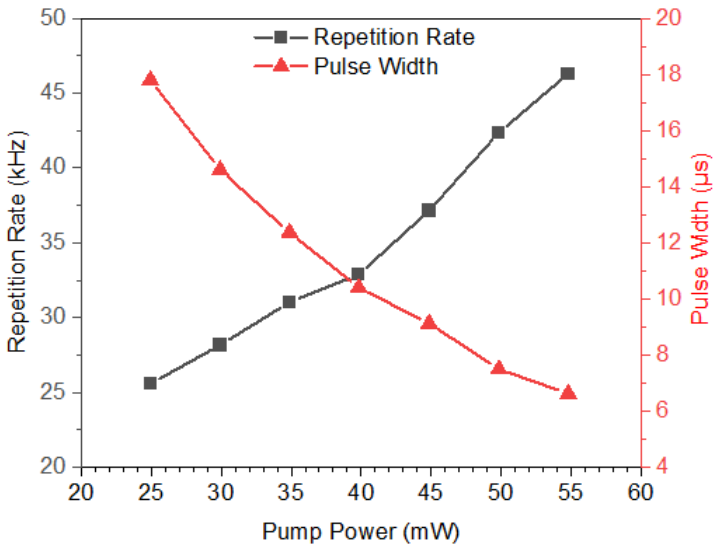


**Fig. 8.** The relation of the repetition rate and pulse width against ascending pump power

Figure 9 shows the variation of average output power, peak power, and pulse energy at different pump power ranging from 25 mW to 55 mW. The output power increase in a linear function from 0.11 to 0.49 mW and the slope efficiency is calculated as 1.3%. The calculated peak power also increases almost in a linear mode, from 0.24 to 1.60 mW. Additionally, the pulse energy rises from 4.34 nJ up to 10.54 nJ.

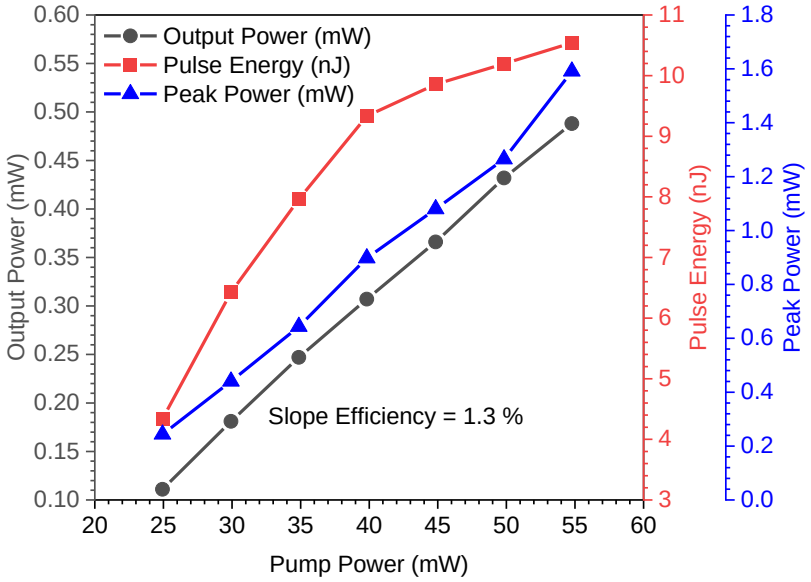


**Fig. 9.** The output power, pulse energy, and peak power of the Q-switched EDFL at different pump power settings

Figure 10 shows the optical spectrum of the output Q-switched laser at 40 mW. The peak intensity of the Q-switched spectrum is -30 dBm and is cantered at 1561 nm. On the other hand, the inset depicts the continuous wave (CW) laser spectrum, without SA in place. The CW laser has a higher peak intensity of -12 dBm and a longer central wavelength of 1567 nm. The Q-switched central wavelength is shifted to the left due to the insertion of SA in the cavity. The SA functions as a loss modulator, that results in population inversion.

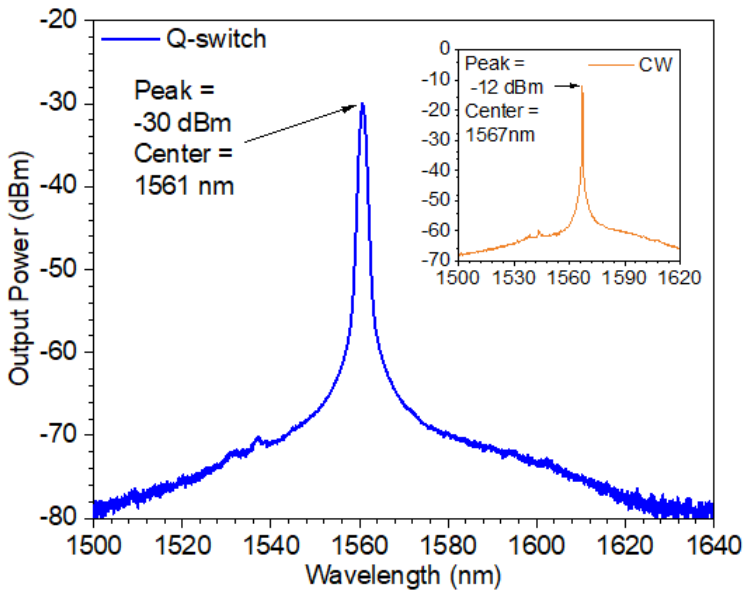


**Fig. 10.** The output spectra of the Q-switched laser and CW laser (inset) at the 40-mW pump power

The sustainability of the Q-switched laser using the fabricated SA was examined under one-hour operation. Figure 11 shows the output spectra taken at a repeated period of 15 minutes and the maximum attainable pump power of 55 mW. As depicted, the output spectra have no significant changes and remain at the same peak of 1561 nm. This suggests that the SA works fine and has not reached the thermal damage threshold. The repeatability of the SA in producing a consistent Q-switched laser was investigated by retesting the SA three times under the same pump power range of 25 mW - 55 mW. The Q-switched laser appeared nearly at the same threshold pump power, with almost the same peak intensity and peak wavelength, indicating good SA reliability.

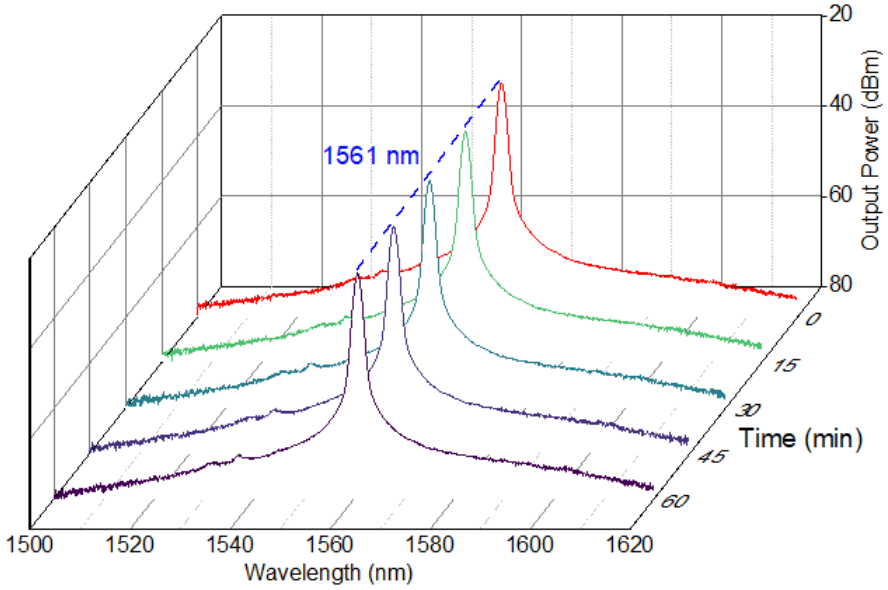


**Fig. 11.** The output spectra that were repeated within 15-minute intervals at 55 mW pump power

Figure 12 shows the pulse train as a time function and is captured at the most attainable pump power of 55 mW. The pulse peak separation (pulse period) is measured as 21.6 µs which is corresponding to a pulse frequency of 46.3 kHz. The pulse's full width at half maximum (FHWM) which is also equivalent to the pulse width is given as 6.6 µs. As shown in the inset, the pulse train for a longer duration (up to 1000 us), shows nearly the same peak intensity, justifying good consistency of the pulse train operating under very small jittering.

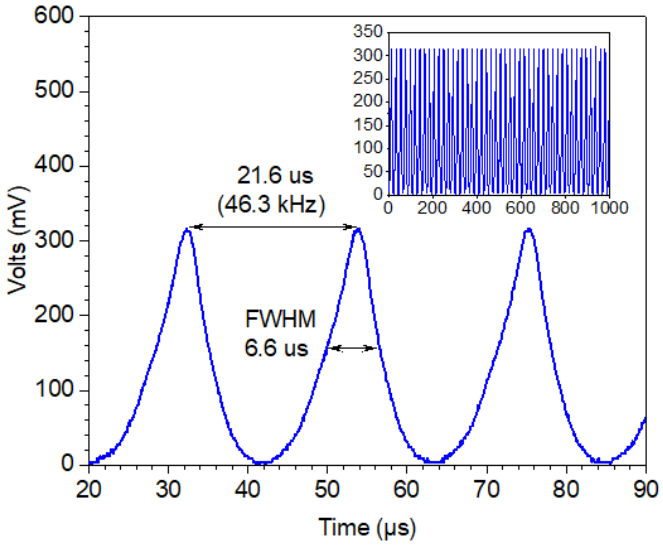


**Fig. 12.** The pulse train with the inset showing pulses within a longer time frame

The RF spectrum (in the frequency domain) which is analyzed at the 40-mW pump power and a resolution bandwidth (RBW) of 250 Hz, is depicted in Figure 13. The fundamental frequency is 32 kHz and it has quite a significant signal-to-noise ratio (SNR) of 49 dB (inset). The RF harmonics also show no significant spectrum damage, which further suggests the stability of the produced Q-switched laser.

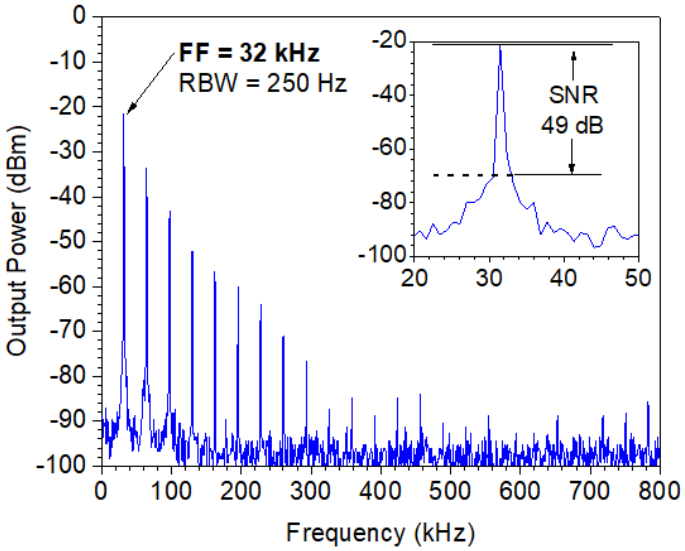


**Fig. 13.** The RF spectrum of the pulsed laser. The inset shows the enlargement of the fundamental frequency spectrum

Table 1 presents the Q-switched output performance, using the $Ti_3Al(C_{0.5}N_{0.5})_2$ SA in comparison with other SA materials. As given in the table, the $Ti_3Al(C_{0.5}N_{0.5})_2$ has a shorter pulse width than the $Fe_3O_4$ [12] and $TM_2O_3$ [22] and has a considerably lower threshold pump power than most of the compared SAs.

**Table 1**
Laser output performance comparison using various SA

| SA Materials | Central wavelength (nm) | Threshold pump power (mW) | Max. Repetition Rate (kHz) | Pulse Width (μs) | Pulse Energy (nJ) | Ref. |
|---|---|---|---|---|---|---|
| $Ti_2AlC$ | 1557 | 86.8 | 29.20 | 2.85 | 92.8 | [21] |
| $Ta_2AlC$ | 1562.128 | 30 | 111.40 | 1.589 | 68.2 | [15] |
| $Fe_3O_4$ | 1560 | 62 | 13.91 | 10.52 | 93.60 | [12] |
| $Ho_2O_3$ | 115.8 | 45 | 115.8 | 0.64 | 0.524 | [13] |
| $Ti_2AlC$ | 1563.4 | 30 | 27.45 | 4.88 | 68.2 | [23] |
| $Tm_2O_3$ | 1563.22 | 81.13 | 62.70 | 9.50 | 6.22 | [22] |
| SCG | 1563 | 16 | 42.23 | 6.40 | 89 | [24] |
| 8-HQCDCL$_2$H$_2$O | 1530 | 50 | 136 | 2.076 | 172 | [25] |
| $Ti_3Al(C_{0.5}N_{0.5})_2$ | 1561 | 24.9 | 46.3 | 6.6 | 10.54 | This study |

## 5. Conclusion

In conclusion, this work has successfully demonstrated a passive single wavelength Q-switched EDFL at 1561 nm by integrating the $Ti_3Al(C_{0.5}N_{0.5})_2$ PVA SA film. The film SA has a linear absorption of 5.7 dB and a modulation depth of 21%. The SA is sandwiched between two ferrules of patch cords and is integrated into the EDFL ring cavity. The Q-switched laser stably appears at 25 mW threshold pump power and sustains up to 55 mW. The maximum operating repetition rate of 46.3 kHz and the shortest pulse width of 6.6 μs are obtained at the 55-mW pump power. Similarly, the highest output power of 0.49 mW, maximum peak power of 1.6 mW, and greatest pulse energy of 10.54 nJ is also achieved at the most attainable pump power of 55 mW. Moreover, uniform pulse shape and intensity are observed for the laser output, with an SNR of 49 dB. The experimental findings show that the MAX phase based on $Ti_3Al(C_{0.5}N_{0.5})_2$ can be a functional saturable absorber.

## Acknowledgement
This work is financially supported by the Ministry of Higher Education Malaysia (MOHE) under FRGS/1/2021/FTKEE/F00489 grant. Additionally, the authors would like to thank the Centre for Telecommunication Research and Innovation (CeTRI), Photonics Engineering Research Group (PERG), Universiti Teknikal Malaysia Melaka (UTeM), and the University of Malaya (UM) for their technical assistance.

## References
[1] Sun, Guoqing, Ming Feng, Kang Zhang, Tianhao Wang, Yuanhao Li, Dongdong Han, Yigang Li, and Feng Song. "Q-Switched and Mode-Locked Er-doped fiber laser based on MAX phase Ti2AlC saturable absorber." *Results in Physics* 26 (2021): 104451. https://doi.org/10.1016/j.rinp.2021.104451

[2] Woodward, Robert I., and Edmund JR Kelleher. "2D saturable absorbers for fibre lasers." *Applied Sciences* 5, no. 4 (2015): 1440-1456. https://doi.org/10.3390/app5041440

[3] Wu, Kan, Bohua Chen, Xiaoyan Zhang, Saifeng Zhang, Chaoshi Guo, Chao Li, Pushan Xiao et al. "High-performance mode-locked and Q-switched fiber lasers based on novel 2D materials of topological insulators, transition metal dichalcogenides and black phosphorus: review and perspective." *Optics Communications* 406 (2018): 214-229. https://doi.org/10.1016/j.optcom.2017.02.024

[4] Rahman, Mohd Fauzi Ab, Anirban Dhar, Shyamal Das, Debjit Dutta, Mukul Chandra Paul, Muhammad Farid Mohd Rusdi, Anas Abdul Latiff, Kaharudin Dimyati, and Sulaiman Wadi Harun. "An 8 cm long holmium-doped fiber saturable absorber for Q-switched fiber laser generation at 2-μm region." *Optical Fiber Technology* 43 (2018): 67-71. https://doi.org/10.1016/j.yofte.2018.04.004

[5] Hamrayev, Hemra, and Kamyar Shameli. "Synthesis and Characterization of Ionically Cross-Linked Chitosan Nanoparticles." *Journal of Research in Nanoscience and Nanotechnology* 7, no. 1 (2022): 7-13. https://doi.org/10.37934/jrnn.7.1.713

[6] Mokhtar, Mohamad Aizad Mohd, Roshafima Rasit Ali, and Eleen Dayana Mohamed Isa. "Silver nanoparticles loaded activated carbon synthesis using clitorea ternatea extract for crystal violet dye removal." *Journal of Research in Nanoscience and Nanotechnology* 3, no. 1 (2021): 26-36. https://doi.org/10.37934/jrnn.3.1.2636

[7] Sukri, Siti Nur Amalina Mohamad, Kamyar Shameli, Sin-Yeang Teow, Eleen Dayana Mohamed Isa, Mostafa Yusefi, and Zatil Izzah Tarmiz. "Short Review: Phytofabrication of zinc oxide nanoparticles for anticancer applications." *Journal of Research in Nanoscience and Nanotechnology* 3, no. 1 (2021): 82-89. https://doi.org/10.37934/jrnn.3.1.8289

[8] Li, Jinjian, Shuoshuo Zhang, Zhidong Bai, Zhongsheng Man, and Shenggui Fu. "Tunable multiwavelength Q-switched erbium-doped fiber laser based on graphene and tapered fiber." *Optical Engineering* 57, no. 9 (2018): 096106-096106. https://doi.org/10.1117/1.OE.57.9.096106

[9] Haris, Hazlihan, Hamzah Arof, Ahmad Razif Muhammad, Carol Livan Anyi, Sin Jin Tan, Nabilah Kasim, and Sulaiman Wadi Harun. "Passively Q-switched and mode-locked Erbium-doped fiber laser with topological insulator Bismuth Selenide (Bi2Se3) as saturable absorber at C-band region." *Optical Fiber Technology* 48 (2019): 117-122. https://doi.org/10.1016/j.yofte.2018.12.002

[10] Woodward, R. I., R. C. T. Howe, T. H. Runcorn, G. Hu, F. Torrisi, E. J. R. Kelleher, and T. Hasan. "Wideband saturable absorption in few-layer molybdenum diselenide (MoSe 2) for Q-switching Yb-, Er-and Tm-doped fiber lasers." *Optics express* 23, no. 15 (2015): 20051-20061. https://doi.org/10.1364/OE.23.020051

[11] Li, Jianfeng, Hongyu Luo, Bo Zhai, Rongguo Lu, Zhinan Guo, Han Zhang, and Yong Liu. "Black phosphorus: a two-dimension saturable absorption material for mid-infrared Q-switched and mode-locked fiber lasers." *Scientific reports* 6, no. 1 (2016): 30361. https://doi.org/10.1038/srep30361

[12] Li, N., H. Jia, M. Guo, J. Zhang, W. Y. Zhang, Z. X. Guo, M. X. Li, Z. X. Jia, and G. S. Qin. "Broadband Fe3O4 nanoparticles saturable absorber for Q-switched fiber lasers." *Optical Fiber Technology* 61 (2021): 102421. https://doi.org/10.1016/j.yofte.2020.102421

[13] Al-Hiti, Ahmed Shakir, Mohd Fauzi Ab Rahman, Sulaiman Wadi Harun, P. Yupapin, and Moh Yasin. "Holmium oxide thin film as a saturable absorber for generating Q-switched and mode-locked erbium-doped fiber lasers." *Optical Fiber Technology* 52 (2019): 101996. https://doi.org/10.1016/j.yofte.2019.101996

[14] Jafry, Afiq Arif Aminuddin, Ahmad Razif Muhammad, Nabilah Kasim, Ahmad Haziq Aiman Rosol, Muhammad Farid Mohd Rusdi, Nik Nurul Nazipah Ab Alim, Sulaiman Wadi Harun, and Preecha Yupapin. "Ultrashort pulse generation with MXene Ti3C2Tx embedded in PVA and deposited onto D-shaped fiber." *Optics & Laser Technology* 136 (2021): 106780. https://doi.org/10.1016/j.optlastec.2020.106780

[15] Ridha, Fay F., Abdul Hadi Al-Janabi, and Ali H. Abdalhadi. "Self-starting Q-switched pulse generation in EDFL ring cavity based on Ta2AlC MAX-phase saturable absorber." *Infrared Physics & Technology* 123 (2022): 104183. https://doi.org/10.1016/j.infrared.2022.104183

[16] Gao, Bo, Ying-Ying Li, Chun-Yang Ma, Yi-Qing Shu, Ge Wu, Bing-Kun Chen, Jia-Yu Huo, Ying Han, Lie Liu, and Ye Zhang. "Ta4C3 MXene as a saturable absorber for femtosecond mode-locked fiber lasers." *Journal of Alloys and Compounds* 900 (2022): 163529. https://doi.org/10.1016/j.jallcom.2021.163529

[17] Ahmad, Harith, Hissah Saedoon M. Albaqawi, Norazriena Yusoff, Wu Yi Chong, and Moh Yasin. "Q-Switched Fiber Laser at $1.5~\mu $ m Region Using Ti 3 AlC 2 MAX Phase-Based Saturable Absorber." *IEEE Journal of Quantum Electronics* 56, no. 2 (2019): 1-6. https://doi.org/10.1109/JQE.2019.2949798

[18] Anasori, Babak, Martin Dahlqvist, Joseph Halim, Eun Ju Moon, Jun Lu, Brian C. Hosler, El'ad N. Caspi et al. "Experimental and theoretical characterization of ordered MAX phases Mo2TiAlC2 and Mo2Ti2AlC3." *Journal of Applied Physics* 118, no. 9 (2015): 094304. https://doi.org/10.1063/1.4929640

[19] Guo, Jia, Huanian Zhang, Chao Zhang, Zhen Li, Yingqiang Sheng, Chonghui Li, Xihao Bao, Baoyuan Man, Yang Jiao, and Shouzhen Jiang. "Indium tin oxide nanocrystals as saturable absorbers for passively Q-switched erbium-doped fiber laser." *Optical Materials Express* 7, no. 10 (2017): 3494-3502. https://doi.org/10.1364/OME.7.003494

[20] Ahmad, Harith, Rabiatul Addawiyah Azwa Tahrin, Nursyafiqa Azman, Syara Kassim, Mohd Afiq Ismail, and Mohd Jamil Maah. "1.5-micron fiber laser passively mode-locked by gold nanoparticles saturable absorber." *Optics Communications* 403 (2017): 115-120. https://doi.org/10.1016/j.optcom.2017.06.094

[21] Sun, Guoqing, Ming Feng, Kang Zhang, Tianhao Wang, Yuanhao Li, Dongdong Han, Yigang Li, and Feng Song. "Q-Switched and Mode-Locked Er-doped fiber laser based on MAX phase Ti2AlC saturable absorber." *Results in Physics* 26 (2021): 104451. https://doi.org/10.1016/j.rinp.2021.104451

[22] Adzimnuddin, M., A. A. Latiff, H. Hazura, M. T. Ahmad, M. A. Azam, and S. W. Harun. "Thulium oxide film as a passive saturable absorber for pulsed fiber laser generation." *Optical Fiber Technology* 58 (2020): 102249. https://doi.org/10.1016/j.yofte.2020.102249

[23] Lee, Jinho, Suhyoung Kwon, and Ju Han Lee. "Ti 2 AlC-based saturable absorber for passive Q-switching of a fiber laser." *Optical materials express* 9, no. 5 (2019): 2057-2066. https://doi.org/10.1364/OME.9.002057

[24] Rusdi, Muhammad Farid Mohd, Afiq Arif Aminuddin Jafry, Anas Abdul Latiff, Ahmad Haziq Aiman Rosol, Mohd Fauzi Ab Rahman, Nabilah Kasim, Muhammad Imran Mustafa Abdul Khudus, Harith Ahmad, and Sulaiman Wadi Harun. "Generation of Q-switched fiber laser at 1.0-, 1.55-and 2.0-µm employing a spent coffee ground based saturable absorber." *Optical Fiber Technology* 61 (2021): 102434. https://doi.org/10.1016/j.yofte.2020.102434

[25] Najm, Mustafa Mohammed, Ahmed Shakir Al-Hiti, Bilal Nizamani, Hamzah Arof, Pei Zhang, Moh Yasin, and Sulaiman Wadi Harun. "Passively Q-switched erbium-doped fiber laser with mechanical exfoliation of 8-HQCDCL2H2O as saturable absorber." *Optik* 242 (2021): 167073. https://doi.org/10.1016/j.ijleo.2021.167073